

Noise and slow-fast dynamics in a three-wave resonance problem

G.D. Lythe and M.R.E. Proctor

*Department of Applied Mathematics and Theoretical Physics,
University of Cambridge, Cambridge CB3 9EW, UK*

Abstract

Recent research on the dynamics of certain fluid dynamical instabilities shows that when there is a slow invariant manifold subject to fast timescale instability the dynamics are extremely sensitive to noise. The behaviour of such systems can be described in terms of a one-dimensional map, and previous work has shown how the effect of noise can be modelled by a simple adjustment to the map. Here we undertake an in depth investigation of a particular set of equations, using the methods of stochastic integration. We confirm the prediction of the earlier studies that the noise becomes important when $\mu |\ln \epsilon| = \mathcal{O}(1)$, where μ is the small timescale ratio and ϵ is the noise level. In addition, we present detailed information about the statistics of the solution when the noise is a dominant effect; the analytical results show excellent agreement with numerical simulations.

Phys.Rev.E **47** 3122-3127 (1993)

1. Introduction

In many circumstances, a low order system of ordinary differential equations (ODEs) serves as a useful model for a physical system. A difficulty arises, however, if the solutions are noticeably affected by small external noise. This is the case in several systems of physical interest sharing the characteristic that their solutions consist of alternating slow and fast phases [1,2,3]. In this paper we take as our example the following third order system of ODEs describing the resonant interaction of three wave modes when one mode is unstable and the other two damped [4,5,6]:

$$\begin{aligned}\dot{x} &= \mu x - y^2 + 2z^2 - \delta z, \\ \dot{y} &= y(x - 1), \\ \dot{z} &= \mu z + \delta x - 2xz.\end{aligned}\tag{1}$$

When μ is small the character of solutions of (1) is dramatically changed by tiny amounts of additive noise – the bifurcation structure with a full gamut of periodic orbits and chaotic regions is replaced by a noisily periodic orbit across a wide range of parameter values (Figure 1). The quantity μ is the ratio of the instability of the unstable mode (its exponential rate of growth in the absence of interaction) to the damping rates of the other two modes (assumed equal). [7]

It is possible to describe the dynamics of (1) in terms of a one-dimensional map. As shown in [1], analytical expressions can be obtained for this map by assuming that the solutions consist of alternating slow and fast phases, and solving approximations to (1) in each phase (Figure 2). In the slow phase the system is close to the invariant plane $y = 0$ and moves slowly from the region where the plane is attracting ($x < 1$) to the region where it is repelling ($x > 1$). This phase is occasionally interrupted by a fast phase which reinjects the system close to the attracting part of $y = 0$. It is in the slow phase that the sensitivity to noise arises.

Here we use a stochastic differential equation to calculate the adjustment to the map of Hughes and Proctor [1] necessary to describe the dynamics of the slow phase in the presence of additive white noise. The smallness of μ is responsible for the division of the dynamics into two phases and the sensitivity to noise. In this paper, all calculations are done to lowest order in μ .

The map we use is a map of successive turning points of x . In the presence of noise the turning point of x which defines the end of the slow phase is a random variable, x_{\max} . In the heuristic model of Hughes and Proctor [1], the noise determines x_{\max} if $\mu |\ln \epsilon| < \mathcal{O}(1)$, where ϵ is the r.m.s. noise level, and x_{\max} is estimated by assuming that $|y| = \mathcal{O}(\epsilon)$ at $x = 1$. The value of x_{\max} calculated in this manner is $\mathcal{O}(1)$ less than the corresponding deterministic value.

In this paper, we extend the treatment of Hughes and Proctor using a stochastic differential equation to describe the slow phase. We derive explicit expressions for

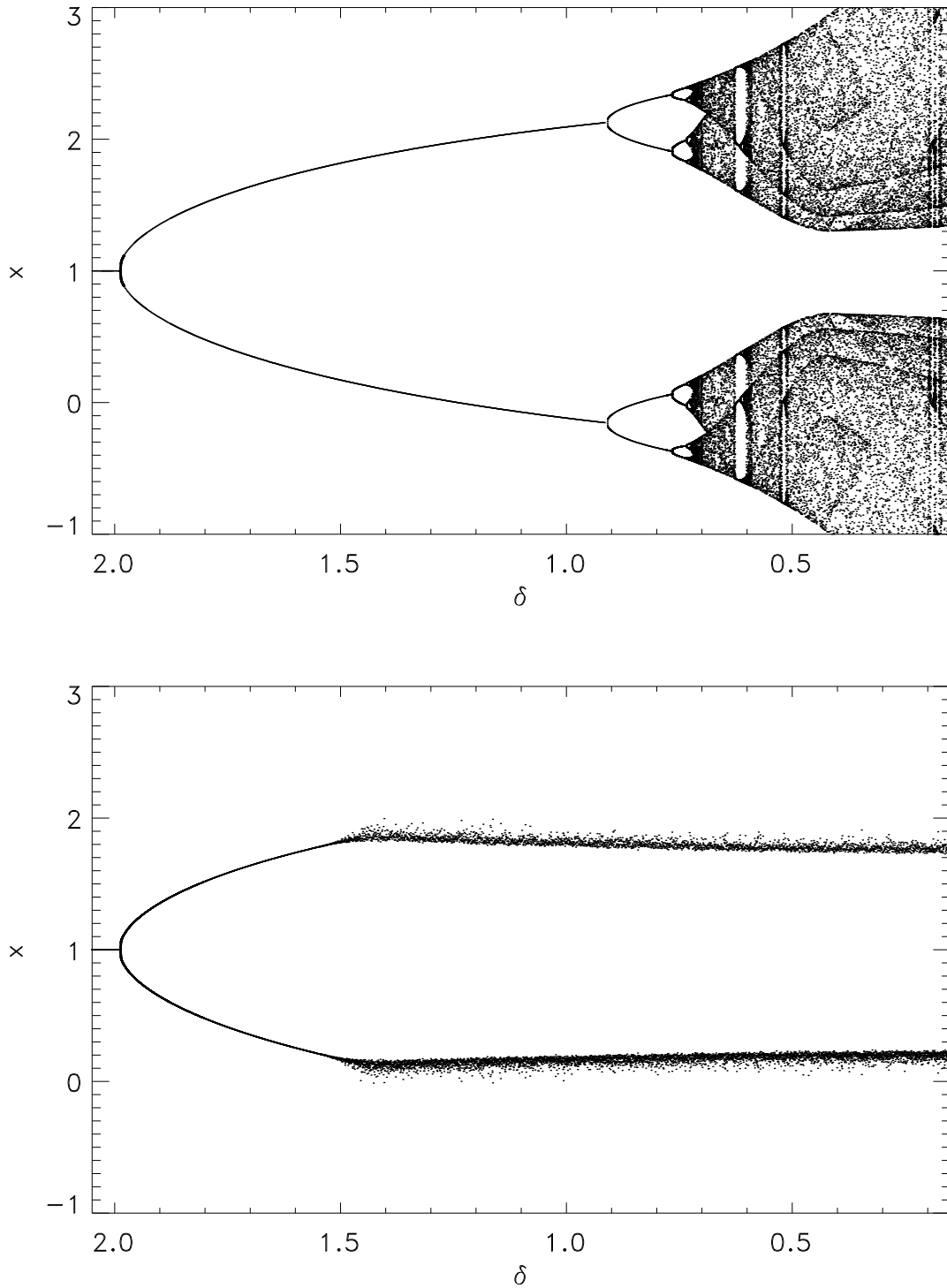


Figure 1. Bifurcation diagrams with and without noise for $\mu = 0.01$. The graphs are obtained from numerical simulation of (1) and each dot represents a turning point of x . The top graph is obtained with no added noise; the bottom graph with very small noise (r.m.s magnitude $\epsilon = 10^{-10}$) added to the variable y . The noiseless bifurcation structure including chaotic regions is replaced by a noisily periodic orbit for $\delta < 1.5$.

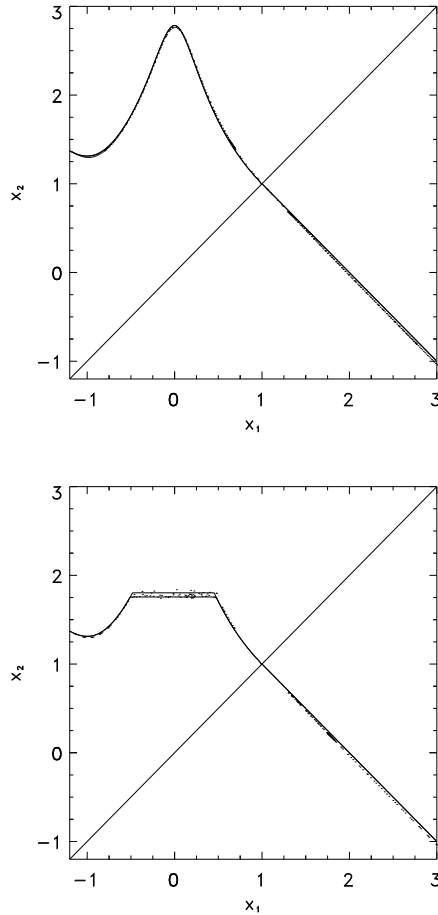


Figure 2. *The one-dimensional map. (If $\dot{x} = 0$ at $x = x_1$ then the next value of x for which $\dot{x} = 0$ is x_2 .) In the top figure, the solid line is the formula of Hughes and Proctor [1] for $\mu = 0.01$ and $\delta = 0.5$. The dots are obtained from numerical solution of (1). The same map is shown below with a flat top due to noise. The two lines in the flat top are $\langle x_{max} \rangle + \sigma_{x_{max}}$ and $\langle x_{max} \rangle - \sigma_{x_{max}}$, calculated as described in the text with $\epsilon = 10^{-10}$, and the dots are numerical results with white noise of magnitude 10^{-10} added to the variable y .*

the probability distribution of x_{\max} , and for the condition on $\mu|\ln \epsilon|$ which marks the transition to the noise-controlled régime. In this régime, the most probable value of x_{\max} is a function of $\mu|\ln \epsilon|$ and the standard deviation of its probability distribution is proportional to μ . For small μ , our calculations predict accurately the results of numerical solution of (1) with low-level noise added to the variable y . The numerical results presented here were obtained using a simple extension of the Heun (second order Runge-Kutta) method for integrating ODEs to include additive white noise [8, 9]. The increment to y at each step includes a Gaussian random variable proportional to ϵ and to the square root of the timestep.

Slow-fast dynamics similar to those of the three-wave resonance system are relevant in other contexts. Our results are presented in a such a way that they can be easily generalised. In the appendix, we show how a generic slow phase is reduced

to a problem taken from dynamic bifurcation theory, and summarise some results for this case.

2. The slow phase with and without white noise

The slow phase of (1) is defined as beginning when the following are true:

$$y^2 \ll \mu, \quad z = \frac{\delta}{2} + \mathcal{O}(\mu), \quad \text{and} \quad \mathcal{O}(\mu) < x < 1. \quad (2)$$

We then find that (1) reduce to:

$$\begin{aligned} \dot{x} &= \mu f(x) - y^2, \\ \dot{y} &= yg(x), \\ z &\simeq \frac{\delta}{2} + \mu \frac{\delta}{4x} \end{aligned} \quad (3)$$

$$\text{where } f(x) = x + \frac{\delta^2}{4x} \quad \text{and} \quad g(x) = x - 1. \quad (4)$$

When the initial conditions (x_0, y_0, z_0) satisfy (2) we observe the following:
 -the variable y decreases exponentially until $x = 1$ and then increases exponentially;
 -the variable x is the driving variable, evolving independently until the very end of the slow phase;
 -the remaining variable, z , is of secondary importance for $x > \mathcal{O}(\mu)$ because it is ‘slaved’ to x (given as a function of x).

Our strategy for determining x_{\max} is to take $\dot{x} = \mu f(x)$, so that x is a function of time, and then solve for y as a function of time. x_{\max} is then the value of x at which $y^2 = \mu f(x)$. The term $-y^2$ in the equation for \dot{x} has a small effect at the end of the slow phase which we calculate a correction for.

In the presence of white noise y becomes a stochastic process y_t satisfying the following stochastic differential equation:

$$dy_t = y_t \tilde{g}(t) dt + \epsilon dW_t \quad (5)$$

where $\tilde{g}(t) = x(t) - 1$, ϵ is a constant with $0 \leq \epsilon \ll \mu$ and W_t is the Wiener process. Exact solution of (5) is possible [10]:

$$y_t = G(t, t_0) \left(y_0 + \epsilon \int_{t_0}^t \frac{1}{G(s, t_0)} dW_s \right) \quad (6)$$

where

$$G(t, t_0) = e^{\int_{t_0}^t \tilde{g}(u) du}. \quad (7)$$

The mean value of y_t ,

$$\langle y_t \rangle = G(t, t_0) y_0, \quad (8)$$

is the solution in the limit $\epsilon \rightarrow 0$. The probability distribution of y is Gaussian with standard deviation, σ_y , a function of time given by

$$\sigma_y^2 = \langle y_t^2 \rangle - \langle y_t \rangle^2 = \epsilon^2 G^2(t, t_0) \int_{t_0}^t \frac{1}{G^2(s, t_0)} ds. \quad (9)$$

If $x = 1$ at $t = t_\alpha$ then for $t - t_\alpha > \mathcal{O}(\frac{1}{\sqrt{\mu}})$

$$\sigma_y^2 \simeq \epsilon^2 \sqrt{\pi a} G^2(t, t_\alpha) \quad (10)$$

where

$$a = \frac{1}{\mu f(1) g'(1)}. \quad (11)$$

2.1. The deterministic limit

If $\sigma_y \ll \langle y_t \rangle$ for $x > 1$ then the noise can be treated as a small perturbation to the deterministic solution given by (8) or by

$$y = y_0 e^{-\frac{1}{\mu}(F(x) - F(x_0))} \quad (12)$$

where

$$F(x) = \frac{1}{2} \ln\left(1 + \frac{4x^2}{\delta^2}\right) - x + \frac{\delta}{2} \tan^{-1}\left(\frac{2x}{\delta}\right). \quad (13)$$

The probability distribution of x_{\max} in this case is very narrow and the mean value, $\langle x_{\max} \rangle$, satisfies

$$F(\langle x_{\max} \rangle) - F(x_0) = \mu \left(\ln y_0 - \frac{1}{2} \ln(\mu f(\langle x_{\max} \rangle)) \right). \quad (14)$$

2.2. The noise-controlled régime

If $\sigma_y \gg \langle y_t \rangle$ for $x > 1$ then it is the noise rather than the initial conditions which controls x_{\max} . In this case the probability distribution of y for $x > 1$ is Gaussian with negligible mean and exponentially rising standard deviation. Equation (10) corresponds to the fact that, for $t - t_\alpha > \mathcal{O}(\frac{1}{\sqrt{\mu}})$, the path of any one realisation is approximately deterministic (but starting from a level which is random variable).

Knowing σ_y as a function of time, we can calculate the probability that y^2 is greater than $\mu f(x)$ at any time. The probability distribution of x_{\max} is the derivative with respect to x of this probability. The probability that x_{\max} lies between x and $x + dx$ is therefore $R(x)dx$ where

$$\begin{aligned} R(x) &= 2 \frac{\partial}{\partial x} \frac{1}{\sqrt{2\pi}\sigma_y} \int_{-\infty}^{-\sqrt{\mu f(x)}} e^{-\frac{y^2}{2\sigma_y^2}} dy \\ &\simeq \frac{2}{\sqrt{2\pi}} \frac{g(x)}{\mu f(x)} \frac{\sqrt{\mu f(x)}}{\sigma_y} e^{-\frac{\mu f(x)}{2\sigma_y^2}}. \end{aligned} \quad (15)$$

The maximum value of $R(x)$ is at $x = \hat{x}$ where \hat{x} is defined by the condition $\sqrt{\mu f(\hat{x})} = \sigma_y$. (Both x and σ_y are functions of time.) Thus \hat{x} satisfies

$$\frac{\sqrt{\mu f(\hat{x})}}{\exp\left(\int_1^{\hat{x}} \frac{g(u)}{\mu f(u)} du\right)} = \epsilon(\pi a)^{\frac{1}{4}} \quad (16)$$

or equivalently

$$F(1) - F(\hat{x}) = \mu |\ln \epsilon| + \frac{\mu}{2} \ln(\mu f(\hat{x})) - \frac{\mu}{4} \ln(\pi a). \quad (17)$$

At the very end of the slow phase the simple relationship $\dot{x} = \mu f(x)$ breaks down because y^2 is no longer negligible. We obtain a more accurate expression for the most probable value of x_{\max} by replacing \hat{x} by $\hat{x}_c = \hat{x} - \Delta\hat{x}$ where

$$\Delta\hat{x} = \int^{x_{\max}} y^2 \frac{dt}{dx} dx \simeq \frac{1}{2} \frac{\mu f(\hat{x})}{g(\hat{x})}. \quad (18)$$

We exhibit the probability distribution of x_{\max} by defining the random variable v as

$$v = -(x_{\max} - \hat{x}_c) \frac{g(\hat{x}_c)}{\mu f(\hat{x}_c)}. \quad (19)$$

The probability that v lies between v and $v + dv$ is $\tilde{R}(v)dv$ where

$$\tilde{R}(v) \simeq \frac{2}{\sqrt{2\pi}} e^v e^{-\frac{1}{2}e^{2v}} \quad (20)$$

which is the probability distribution of the log of the absolute value of a Gaussian random variable with unit variance. Explicit expressions for the mean and variance of v exist:

$$\langle v \rangle = -\frac{1}{2}(\gamma + \ln 2) \quad (21)$$

where $\gamma = .577\dots$ (Euler's constant) and

$$\langle v^2 \rangle - \langle v \rangle^2 = \frac{\pi^2}{8} \quad (22)$$

so the mean and standard deviation of x_{\max} in the noise-controlled régime are given by

$$\langle x_{\max} \rangle = \hat{x}_c + \frac{1}{2} \frac{\mu f(\hat{x}_c)}{g(\hat{x}_c)} (\gamma + \ln 2) \quad (23)$$

$$\sigma_{x_{\max}} = \sqrt{\langle x_{\max}^2 \rangle - \langle x_{\max} \rangle^2} = \frac{\pi}{2\sqrt{2}} \frac{\mu f(\hat{x}_c)}{g(\hat{x}_c)}. \quad (24)$$

Each value of x_1 for $-1 + \mathcal{O}(\sqrt{\mu}) < x_1 < 1$ in Figure 2 corresponds to a set of initial conditions for the slow phase [1]. The value taken for x_2 is the lower of the two values given by (14) and (23). When the noise-controlled value (23) is the lower, we plot $\langle x_{\max} \rangle + \sigma_{x_{\max}}$ and $\langle x_{\max} \rangle - \sigma_{x_{\max}}$. For the purposes of Figure 2, the transition from the noise-controlled to the deterministic régime is sufficiently rapid that it is unnecessary to consider the transition region. In the next section, however, we derive a more general formula for the probability distribution of x_{\max} .

2.3. A more general formula

We express the relative magnitudes of the deterministic and noise-driven parts of y_t via the parameter c defined as

$$c = \frac{\langle |y_t| \rangle}{\sigma_y} \quad (25)$$

which is constant for $t - t_\alpha > \mathcal{O}(\frac{1}{\sqrt{\mu}})$ (10). The noise-controlled régime corresponds to $0 < c \ll 1$, and the deterministic limit to $c \gg 1$. The condition $c < 1$ for $t - t_\alpha > \mathcal{O}(\frac{1}{\mu})$ can be taken as a test of whether the noise-controlled régime is in force. This condition is

$$\mu |\ln \epsilon| < F(1) - F(x_0) + \mu \left(\frac{1}{4} \ln(\pi a) - \ln y_0 \right). \quad (26)$$

A more general formula for $R(x)$ is obtained by allowing the probability distribution of y for $x > 1$ to have non-zero mean. Thus

$$\begin{aligned} R(x) &= \frac{\partial}{\partial x} \frac{1}{\sqrt{2\pi}\sigma_y} \int_{-\sqrt{\mu f(x)}}^{\sqrt{\mu f(x)}} e^{-\frac{(y - \langle y \rangle)^2}{2\sigma_y^2}} dy \\ &\simeq \frac{1}{\sqrt{2\pi}} u \left(e^{-\frac{1}{2}(u-c)^2} + e^{-\frac{1}{2}(u+c)^2} \right) \frac{g(x)}{\mu f(x)} \end{aligned} \quad (27)$$

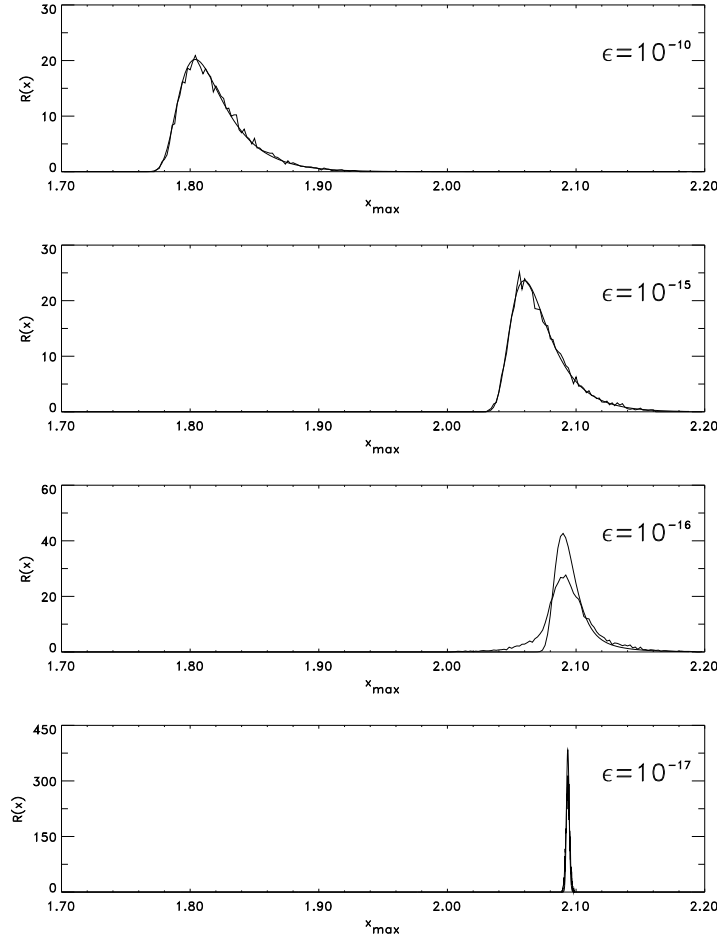


Figure 3. *The effect of noise on the probability distribution of x_{max} . Numerically-obtained probability distributions of x_{max} with $\mu = 0.01$ and $\delta = 1.0$. The smooth curve in each case is the function $R(x)$ (27) which reduces to (15) in the noise-controlled régime.*

where

$$u = \frac{\sqrt{\mu f(x)}}{\sigma_y}. \quad (28)$$

This probability distribution is compared with numerical results for $\mu = 0.01$ in Figure 3. In the limit $c \rightarrow 0$ we find the distribution (20). For large c we regain the deterministic régime (narrow, Gaussian distribution of x_{max}).

Our results are exact for small μ and delta function initial conditions. To produce Figure 3 and Figure 4 we take the initial conditions from the corresponding deterministic orbit. This gives excellent agreement in the noise-controlled régime, where x_{max} is independent of initial conditions, and gives the correct large- c limit for $\langle x_{max} \rangle$. However the standard deviation $\sigma_{x_{max}}$ is underestimated for nonzero c because the probability distribution of x_{max} is carried through the fast phase, so the initial conditions for the slow phase vary from cycle to cycle in the noisily periodic orbit. The broadening of the probability distribution of x_{max} produced

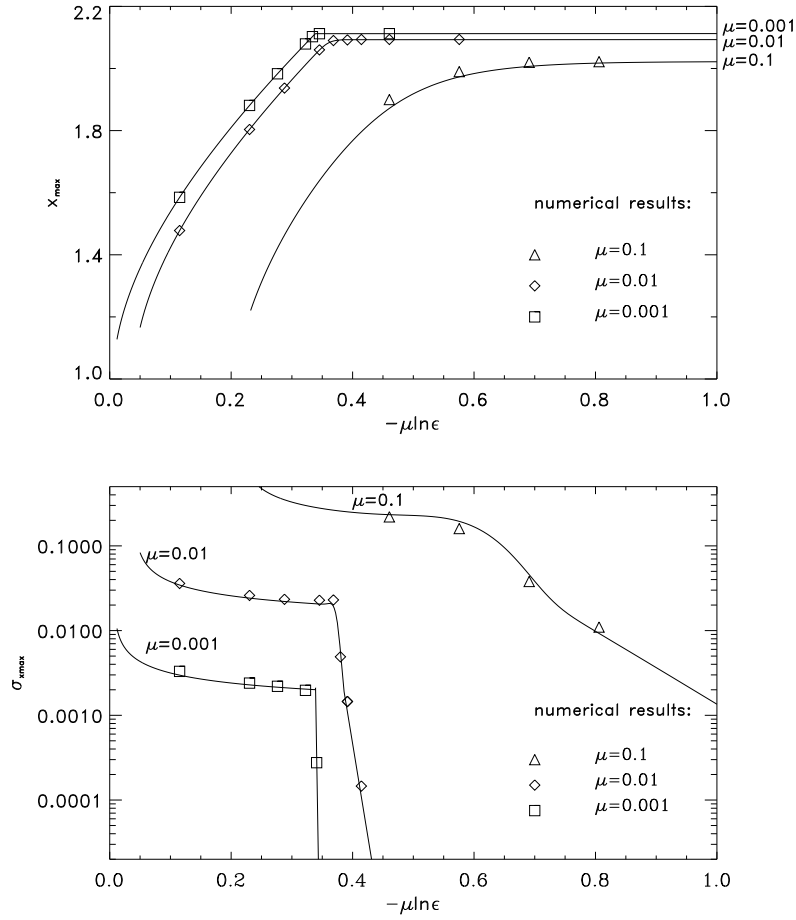


Figure 4. Mean and standard deviation of x_{\max} as a function of $\mu|\ln \epsilon|$. The curves are predictions obtained from the explicit form for the probability distribution of x_{\max} (27) and some numerical results are shown. The agreement between small- μ calculations and numerical results is good even for μ as large as 0.1. The knee in the graph of $\sigma_{x_{\max}}$ vs $\mu|\ln \epsilon|$ corresponds to the end of the noise-controlled régime.

by this is most noticeable in the transition region between the noise-controlled and deterministic régimes ($\epsilon = 10^{-16}$ in Figure 3).

In Figure 4 we compare numerical results for the most probable value of x_{\max} and the standard deviation of x_{\max} with values calculated using the explicit form of the probability distribution (27). The most probable value of x_{\max} we find from the (approximate) condition

$$u^2 = 1 + c^2. \quad (29)$$

This corresponds to $\langle y_t^2 \rangle = \mu f(x)$ and gives the correct result in the large and small c limits. The standard deviation of x_{\max} can be written

$$\sigma_{x_{\max}} \simeq \frac{\pi}{2\sqrt{2}} \frac{\mu f(x)}{g(x)} h(c) \quad (30)$$

where $f(x)$ and $g(x)$ are evaluated at the most probable value of x_{\max} , $h(0) = 1$ and, for large c , $h(c) \simeq \frac{1}{c}$. The form we have used for $h(c)$ in Figure 4 is $h^2(c) = \frac{1}{1+c^2} + c^2 e^{\frac{-c^2}{1.5}}$, which we obtained as a fit to numerical integration of (27).

3. Conclusion

Slow-fast dynamical systems such as the three-wave resonance system discussed here are most conveniently described in terms of a one-dimensional map. Low-level white noise has an $\mathcal{O}(1)$ effect true which can be calculated by solving a stochastic differential equation. In the deterministic limit x_{\max} , the turning point of x which defines the end of the slow phase, is determined by the initial conditions. In the noise-controlled régime, which is in force when $\mu |\ln \epsilon|$ is less than an $\mathcal{O}(1)$ constant which depends on initial conditions, x_{\max} is a random variable with most probable value a function of $\mu |\ln \epsilon|$ and standard deviation proportional to μ .

We know of several other physical contexts which give rise to noise-sensitive slow-fast dynamics. One is the shear instability of tall thin convection cells [2, 3]. Another is pulsating laser oscillations [11, 12] consisting of short pulses separated by long periods of very small intensity. A related problem is that of random perturbations of heteroclinic attractors [13], where noise controls the length of time spent near an unstable fixed point, and a stable homoclinic or heteroclinic orbit provides the reinjection.

Acknowledgement

G.L. is grateful for financial support from the Commonwealth Scholarship Commission.

Appendix

In the three-wave resonance problem considered above, the slow phase is defined by

$$\begin{aligned} \dot{x} &= \mu f(x), \\ dy_t &= g(x)y_t dt + \epsilon dW_t \end{aligned} \tag{31}$$

where $f(x) = x + \frac{\delta^2}{4x}$ and $g(x) = x - 1$. We obtain a system often studied in dynamic bifurcation theory [14] if we put $f(x) = 1$ and $g(x) = x$. Then y_t satisfies

$$dy_t = g(t)y_t dt + \epsilon dW_t \quad \text{where } g = \mu t \tag{32}$$

Suppose $y = y_0$ for some $t = t_0 < 0$. (In the three-wave resonance problem the natural choice is $y_0 = \mathcal{O}(\sqrt{\mu})$ and $-\mu t_0 = \mathcal{O}(1)$.) The next value of g at which $y = y_0$, \bar{g} , defines a dynamic bifurcation point, occurring later than the ‘static’ bifurcation at $g = 0$. In fact, in the deterministic limit, $\bar{g} = -g(t_0)$.

The noise-controlled régime is in force if

$$\mu |\ln \epsilon| < \frac{1}{2} g^2(t_0) + \mu \left(\frac{1}{4} \ln \frac{\pi}{\mu} - \ln y_0 \right). \tag{33}$$

In this régime, \bar{g} is a random variable with most probable value, \hat{g} , given by

$$\hat{g}^2 = 2\mu|\ln \epsilon| + \frac{\mu}{2} \ln \frac{\mu}{\pi} + 2\mu \ln y_0 \quad (34)$$

and standard deviation $\sigma_{\bar{g}}$ by

$$\sigma_{\bar{g}} = \mu \frac{\pi}{2\sqrt{2}} \frac{1}{\hat{g}}. \quad (35)$$

In this form, our results appear consistent with results obtained numerically [15], from an electronic circuit model of a ring laser [16] and with analytical results for the laser threshold instability [17].

References

- [1] D.W. Hughes and M.R.E. Proctor “Chaos and the effect of noise in a model of three-wave mode coupling.” *Physica D* **46** 163–176 (1990).
- [2] D.W. Hughes and M.R.E. Proctor “A low order model of the shear instability of convection: chaos and the effect of noise.” *Nonlinearity* **3** 127–153 (1990).
- [3] M.R.E. Proctor and D.W. Hughes “The false Hopf bifurcation and noise sensitivity in bifurcations with symmetry.” *Eur.J.Mech.,B/Fluids* **10** 81–86 (1990).
- [4] S.Ya. Vyshkind and M.I. Rabinovich “The phase stochastization mechanism and the structure of wave turbulence in dissipative media.” *Sov. Phys. JETP* **44** 292–299 (1976).
- [5] J.-M. Wersinger, J.M. Finn and E. Ott “Bifurcation and “strange” behaviour in instability saturation by nonlinear three-wave mode coupling.” *Phys. Fluids* **23** 1142–1154 (1980).
- [6] Jean-Marie Wersinger, John M. Finn and Edward Ott “Bifurcations and strange behaviour in instability saturation by nonlinear mode coupling.” *Phys. Rev. Lett.* **44** 453–457 (1980).
- [7] The change of variables from the equations for the amplitudes of the three wave modes used here differs from that of Hughes and Proctor; our (x, y, z) corresponds to $(-x, w, y)$.
- [8] Rebecca L. Honeycutt “Stochastic Runge-Kutta algorithms. I. White noise.” *Phys. Rev. A* **45** 600–603 (1992).
- [9] Peter E. Kloeden and Eckhard Platen, *Numerical Solution of Stochastic Differential Equations* (Springer, Berlin, 1992).
- [10] C.W. Gardiner, *Handbook of Stochastic Methods* (Springer, Berlin, 1990).
- [11] Paul Mandel and T. Erneux “Laser Lorenz equations with a time-dependent parameter.” *Phys. Rev. Lett.* **53** 1818–1820 (1984).
- [12] Miltiades Georgiou and Thomas Erneux “Pulsating laser oscillations depend on extremely-small-amplitude noise.” *Phys. Rev. A* **45** 6636–6642 (1992).
- [13] Emily Stone and Philip Holmes “Random perturbations of heteroclinic attractors.” *SIAM J. Appl. Math.* **50** 726–743 (1990).
- [14] E. Benoît (Ed.), *Dynamic bifurcations* (Springer, Berlin, 1991).
- [15] G. Broggi, A. Colombo, L.A. Lugiato and Paul Mandel “Influence of white noise on delayed bifurcations.” *Phys. Rev. A* **33** 3635–3637 (1986).
- [16] R. Mannella, Frank Moss and P.V.E. McClintock “Postponed bifurcations of a ring-laser with a swept parameter and additive colored noise.” *Phys. Rev. A* **35** 2560–2566 (1987).
- [17] M.C. Torrent and M. San Miguel “Stochastic-dynamics characterization of delayed laser threshold instability with swept control parameter.” *Phys. Rev. A* **38** 245–251 (1988).